JVST A
Journal of Vacuum Science & Technology A

Assessment of atomic layer deposited TiO_2 photocatalytic self-cleaning by quartz crystal microbalance

Cite as: J. Vac. Sci. Technol. A **38**, 043404 (2020); https://doi.org/10.1116/6.0000198
Submitted: 16 March 2020 . Accepted: 19 May 2020 . Published Online: 02 June 2020

Théo Henry, Paolo Martins, Etienne Eustache, Bernard Servet, Laurent Divay, Pierre Jouanne, Philippe Grasset, Jean-Paul Dudon, Patrick Hugonnot, and Karl Fleury-Frenette

JVST A
Journal of Vacuum Science & Technology A

ARTICLE

avs.scitation.org/journal/jva

Assessment of atomic layer deposited TiO_2 photocatalytic self-cleaning by quartz crystal microbalance

Cite as: J. Vac. Sci. Technol. A 38, 043404 (2020); doi: 10.1116/6.0000198
Submitted: 16 March 2020 · Accepted: 19 May 2020 ·
Published Online: 2 June 2020

Théo Henry,[1,a)] Paolo Martins,[2] Etienne Eustache,[2] Bernard Servet,[2] Laurent Divay,[2] Pierre Jouanne,[3] Philippe Grasset,[3] Jean-Paul Dudon,[3] Patrick Hugonnot,[3] and Karl Fleury-Frenette[1,b)]

AFFILIATIONS

[1]Surface Micro & Nano Engineering Laboratory, Centre Spatial de Liège (CSL), Space Sciences, Technologies and Astrophysics Research (STAR) Institute, University of Liège, Avenue du Pré-Aily, Liege Science Park, B29 4031 Angleur, Belgium
[2]Thales Research & Technology France, Campus Polytechnique, 1 avenue Augustin Fresnel, 91767 Palaiseau Cedex, France
[3]Thales Alenia Space, 5 Allée des Gabins BP99, 06156 Cannes La Bocca Cedex, France

[a)]**Electronic mail:** thenry@uliege.be
[b)]**Electronic mail:** kfleury@uliege.be

ABSTRACT

The self-cleaning properties emerging from photocatalytic effects consist in the elimination of an organic contamination layer by light-induced redox reactions. Quartz crystal microbalances (QCMs), monitoring the contaminant mass loss under UV illumination, were used to investigate this effect and its efficiency. A new setup dedicated to such purpose is introduced along with the results of a self-cleaning experiment performed with a 20-nm TiO_2 thin film coated on a QCM by atomic layer deposition. In particular, a 10-nm paraffin oil thin film deposited under vacuum is shown to be degraded down to its complete removal according to a zeroth order photocatalytic reaction. Finally, the experimental opportunities offered by the new setup, such as a controlled environment composition, are presented.

I. INTRODUCTION

The self-cleaning properties driven by photocatalysis have attracted a lot of attention and research up to now. When irradiated with wavelengths below the semiconductor bandgap, an electron-hole pair is produced. The created charge carriers can be trapped, be recombined, or interact with surface species leading to potential redox reactions and eventually to organic molecule degradation. Such ability allows the development of a large variety of applications[1–4] such as water treatment,[5,6] air cleaners,[7–9] antibacterial effect,[10,11] or self-cleaning surfaces.[12–14] When the semiconductor valence and conduction bands allow it, the redox reactions are often favored by the generation of reactive oxygen species (ROS) being mainly[1–3,15,16] O_2^-, OH, and H_2O_2 through the reaction of H_2O and O_2 present in the atmosphere (or solvent). Overall, a wide range of organics can be decomposed.[16–20] For self-cleaning surfaces, the light-induced super hydrophilicity phenomenon[1–3,12,14] also contributes to cleaning by spreading water over the surface, limiting organic contamination and removing dust particles. Wang *et al.*[21,22] attribute it to the formation of vacant oxygen sites through metallic atom reduction helping water dissociation and increasing water spreading. This was also found for hydrocarbons.[21,22] This effect is not occurring for all photocatalytic materials.[23]

Self-cleaning ability governed by photocatalytic decomposition is often studied by UV-VIS spectroscopy or reaction product analysis with chromatographic methods. Such techniques are proposed by ISO standards,[4] but they do not characterize the contaminant itself. On one hand, chromatography infers the presence of a photoreaction through the identification of desorbed reaction products. On the other hand, UV-VIS spectroscopy relies on an optical response that can be influenced by other factors than the amount of adsorbed contaminant on the surface alone such as, for instance, UV-induced changes in the contaminant optical properties or interferential effects involving the underlying coating and substrate. Both methods cannot unequivocally ascertain the extent of the

contaminant removal. Another widespread method is monitoring the self-cleaning behavior through contact angle measurements as described in the ISO 27448 standard.[24] Nevertheless, the method again does not provide direct information on the contaminant removal behavior because the decrease in contact angle starts to occur mainly when only a small amount of contaminant remains on the surface.[4] Moreover, a significant contact angle drop does not necessarily mean that the contaminant is completely eliminated.

The use of quartz crystal microbalances is particularly well suited to overcome these limitations by allowing to monitor the contaminant photo-induced mass changes and thus the ensuing self-cleaning effect. Several studies of the photocatalytic activity of thin films by quartz crystal microbalance (QCM)[25–35] or QCM-D[36–39] were conducted. They mainly dwell on TiO_2 deposited by sol-gel methods,[26,27,31,32,34] liquid routes,[30,33] atomic layer deposition (ALD),[37] or reactive magnetron sputtering.[36,38] The reactions are studied in aqueous media[25–30,36–39] or in air with a contaminant either in the solid phase,[32] gas phase,[35] or deposited by the liquid route[31,33,34,37] with film thickness ranging from 60 nm to more than 1 μm.

Here, a new setup is presented for photocatalytic experiment from the contamination phase up to the irradiation phase in air or N_2. It consists of a vacuum chamber equipped with an effusion cell, QCMs, and irradiation system. With a short set of experiments, we demonstrate the photocatalytic activity of a 20-nm anatase TiO_2 thin film (to our knowledge, this is the thinnest such film studied with QCMs) deposited by ALD by showing its ability to remove 10 nm of hydrocarbons in approximatively 1 h and thus demonstrating its effectiveness as "self-cleaning coating" in air. In addition, this effect is not observed under N_2. Furthermore, different experimental perspectives offered by the introduced setup are presented.

II. EXPERIMENT

A. Experimental and setup description

The experimental setup, schematically displayed in Fig. 1, briefly consists in two QCMs mounted in a high vacuum chamber equipped with an effusion cell and UV illumination capability. Contamination deposition and UV exposure can be carried out at pressure from 1 atm down to 5×10^{-8} mbar. The chamber can be isolated from the pumping system with a solenoid valve. Air venting can be either instantaneous or progressive with a manual valve. QCMs are AT-cut 6 MHz crystals with Cr/Au electrodes (theoretical resolution of 0.03 Hz equivalent to 3.7×10^{-3} nm for a material density of 1 g cm^{-3}). The QCM deposition rate monitor is a STM-2 from Inficon. Precision of reported values are estimated at ±0.1 nm. QCMs are cooled with a water-glycol solution. Temperature is monitored during the experiment using a K-type thermocouple fixed to the main QCM head (QCM_1). A MgF_2 transmission window allows to illuminate the QCMs with an external source.

The illumination device is an OmniCure® S2000 Spot UV Curing System (Excelitas Technology) combined with a 400-nm Techspec® lowpass filter of OD > 4.0. Its spectrum is displayed in Fig. 2. Irradiance is measured with an UV-Optometer from SUSS MicroTech over the 349–385 nm range. The effusion cell for contamination deposition is a leak valve made of an Incoloy heat cartridge (200 W) with an integrated J-type thermocouple connected to the main chamber with a feedthrough. Such a system allows for heating the contaminant up to 600 °C and controlling deposition rates down to 0.01 nm s^{-1} (see Sec. II C Fig. 3).

Paraffin oil from Merck (CAS 8012-95-1) with a density of 0.86 g cm^{-3} and boiling temperature around 300 °C is used in the present study. In liquid phase at ambient temperature, it consists mainly of branched hydrocarbon chains with naphthenic compounds. Its absorption spectrum measured with a Perkin Elmer Lambda 950 spectrometer in 1 cm thick PMMA cell is displayed in Fig. 2. Its absorption coefficient is 0.027 cm^{-1}. The absorption peak below 300 nm originates from naphthenic compounds.[40]

B. Tio_2 ALD deposition and characterization

TiO_2 thin films were deposited on a QCM with $TiCl_4$ and H_2O precursors at 270 °C using a BENEQ TFS 200 system. A process of 440 cycles was performed in order to reach a coating thickness of 20 nm. Each cycle is composed of one pulse of $TiCl_4$

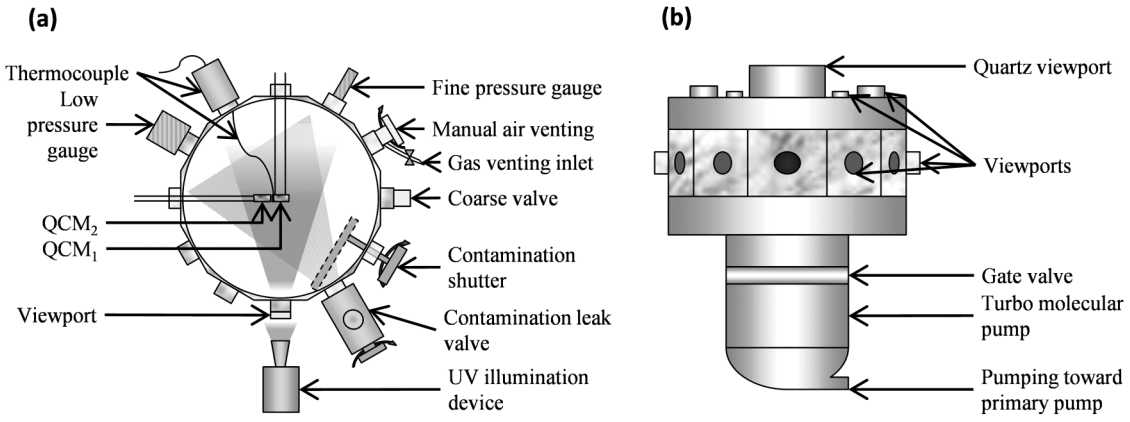

FIG. 1. Vacuum chamber: (a) top view; (b) side view.

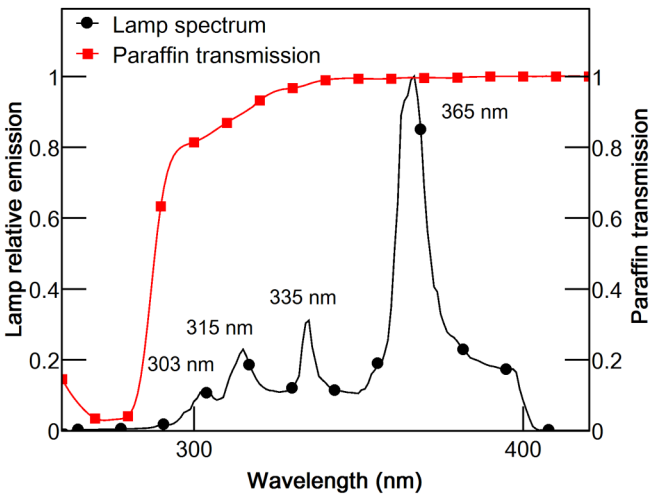

FIG. 2. Spectrum of the used illumination system and the contaminant transmission.

(300 ms) with a purge time of 5 s and one pulse of H_2O (150 ms) with a purge time of 5 s. Coatings were also performed on silicon (100) substrates in the same ALD batch to be used as witness samples. ALD allows crystalline metal oxide synthesis at relatively low temperatures.[41] It is based on surface chemistry providing an excellent control of thin film thickness at nanoscale with high uniformity/conformability depositions over large areas or complex topographies.[42,43] Spectroscopic ellipsometry (SE) using a Sentech SE 800 ellipsometer was used for thickness determination. Multiple angle measurements were performed at 60°, 65°, and 70° between 330 and 820 nm. The crystalline phase of the deposit was identified by Raman spectroscopy using an Invia Renishaw microspectrometer system and by x-ray diffraction using (XRD) a Panalytical Empyrean Diffractometer delivering Cu Kα radiation. The surface topography of the samples was inspected by scanning electron microscopy (SEM) using a Zeiss Sigma HD system.

C. Photocatalytic experiment methodology

For photocatalytic experiments, 10 nm of paraffin oil was deposited at 1.6×10^{-6} mbar at 0.025–0.030 nm s^{-1} on TiO_2/Au-coated QCM. An example of deposition rate stability based on QCM measurements is discussed here below. Directly after deposition; the chamber is isolated from the pumping system and then vented to atmospheric pressure. Once reached, a short period of time is required for the pressure and temperature measurements to stabilize before the UV irradiation is turned on. The QCMs cooling temperature is set to 15 °C during the complete experiment to avoid thermal desorption and mass uptake by water condensation. The maximum temperature difference between the two QCMs is 1 °C along the whole experiment and 0.1 °C during steps under vacuum. For QCM measurements, the contaminant density is set to 1 g cm^{-3} since the outgassing product density is unknown. Thanks to the Sauerbrey's equation [Eqs. (1) and (2)], the frequency shift can then be expressed as mass or thickness as follows where Δf (Hz) is the normalized frequency change, f_0 (Hz) is the resonant frequency of the fundamental mode, A is the piezoelectrically active crystal area (cm^2), ρ_q is the quartz density (2.648 g cm^{-3}), μ_q is the shear modulus of quartz (2.947×10^{11} g cm^{-1} s^{-2} for AT-cut crystal), and Δm is the mass change (g),

$$\Delta f = -\frac{2f_0^2}{A\sqrt{\rho_q \mu_q}}\Delta m, \tag{1}$$

$$\Delta f \approx -2.26.10^{-6} f_0^2 \frac{\Delta m}{A}. \tag{2}$$

The so-called "z" value arising from the "z-match" method aiming to compensate shift frequency induced by the differences of acoustic impedance and shear properties between the quartz crystal and the deposited material is again set to 1 since no reference data

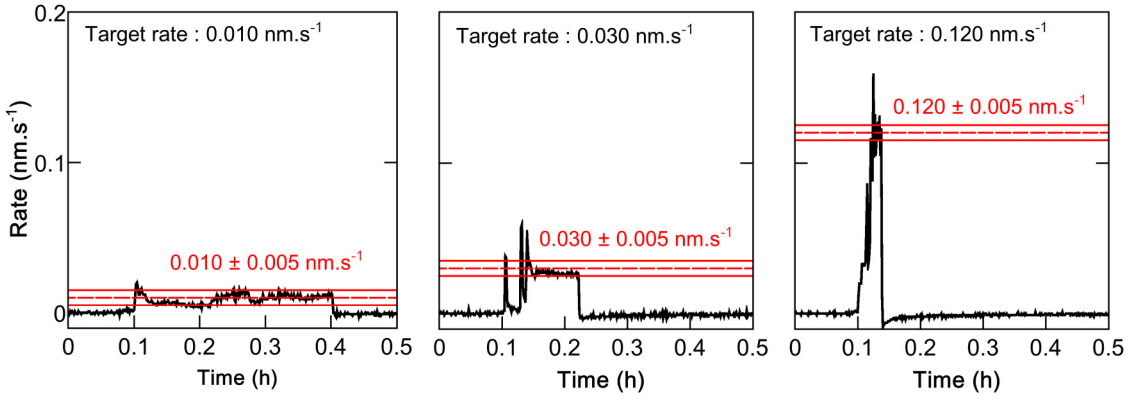

FIG. 3. Deposition rate stability measured by the QCM monitor with a density of 1 g cm^{-3} and a z-ratio of 1 for different target rates. The deposition was stopped when the QCM monitor indicated that 10 nm of paraffin oil was reached.

are known for the used contaminant. Typical z-ratio values of several materials can be found in Ref. 44. They range from 0.13 up to 5.6. Taking into account impedance matching, the mass change is now given[45,46] by [Eq. (3)], where N_q is the frequency constant for the AT-cut quartz crystal [Eq. (4)], Z is the z-ratio [Eq. (5)] expressed as the function of the density and the shear modulus of the quartz [ρ_q and μ_q] and the deposited thin film (ρ_f and μ_f), f_L is the crystal frequency loaded with the deposited thin film, and f_U is the frequency of the unloaded crystal,

$$\frac{\Delta m}{A} = \left(\frac{N_q \rho_q}{\pi Z f_L}\right) \tan^{-1}\left[Z \tan\left(\pi\left(\frac{f_U - f_L}{f_U}\right)\right)\right] \quad (3)$$

with

$$N_q = \frac{\sqrt{\rho_q \mu_q}}{2\rho_q} \quad (4)$$

and

$$Z = \sqrt{\left(\frac{\rho_q \mu_q}{\rho_f \mu_f}\right)}. \quad (5)$$

However, when the frequency shift induced by mass deposition is lower than 2%–5%,[45–47] as it is the case for this study, the Sauerbrey's equation without z correction is considered to provide precise thickness values. Some limitations for given materials can be found in the works of Benes.[48] For the used 6 MHz quartz crystal, 2% corresponds to 0.12 MHz leading to 14.7 μm for a material having a density of 1 g cm^{-3}. As example of validity, Behrndt[49] found a clear linear relation between the measured mass with a 5 MHz crystal oscillator and weighting up to more than 12.5 μm. In the present case, the deposition of 10 nm of paraffin oil would induce a shift of only 81.4 Hz considering Saeubrey's equation with a material density of 1 g cm^{-3}. When the deposition of paraffin oil is performed, a shift of 82 Hz is measured ensuring that the TiO_2 layer does not affect the estimated thickness of the contaminant. The term of QCM thickness reading would be more appropriate here in view of the above assumptions on the deposited material density and default z-value, but thickness will be used in the text for the sake of simplicity. Note that the target deposited thickness (10 nm) is set for the TiO_2/Au-coated QCM placed in front of the irradiation source and the closest to the effusion cell outlet. It will be referred to as "QCM_1" and the second one with a reference Au-coated crystal as "QCM_2." Both QCMs are exposed to different amounts of contaminant and thus measure different thicknesses in reason of their position with respect to the effusion cell. The contaminant deposition ratio QCM_2/QCM_1 is approximately 0.75. The illumination is normal with respect to QCMs. The measured flux is 12 mW cm^{-2} for QCM_1. The QCM_2 receives approximatively 90% of the flux seen by QCM_1. Mass and temperature measurements are integrated over 5 s. The room temperature is 25.0 °C ± 1.0 °C with a relative humidity of 33 ± 2%.

III. RESULTS AND DISCUSSION

A. TiO_2 coating characterization

Figure 4 shows the Raman spectrum of coated QCM. The gold underlayer contribution was subtracted by post-treatment. The Raman peaks correspond to the anatase phase of TiO_2.[50,51]

The anatase phase is also confirmed by XRD. QCMs are composed of a polycrystalline gold film deposited on a quartz crystal. In order to clearly identify the phase of the TiO_2 thin film, the sample was tilted for the measurement at $\omega = 5°$ with reference of the quartz <101> direction (ICDD PDF 00-046-1045). Indeed, without this precaution, we found that anatase (101) planes (ICDD PDF 00-021-1272) diffracting at $2\theta = 25.3°$ are hidden by exalted quartz (101) planes diffracting at $2\theta = 26.6°$. The resulting diffractogram of TiO_2 coated QCM is shown in Fig. 5. A small residue of quartz is found for its (101) plane. The observable significant peaks at 38.2°, 44.4°, and 64.6° correspond to the gold film (ICDD PDF 00-004-0784). We also observed smaller peaks, most noticeably at 25.3° and 48.0°. These peaks are characteristic of the anatase phase of TiO_2, being, respectively, the diffracting planes (101) and (200). It corroborates the conclusions of Raman spectroscopy experiment. No evidence of other phase is detected.

From SEM images (Fig. 6), the TiO_2 coating seems to preserve Au-QCM topography at large scale (x1000). At high magnification, the large gold grains disappear, covered by small anatase grains. They are covering the entire surface, even in Au grain boundaries, furrows, and particle edges [Figs. 6(e) and 6(f)].

Because the QCM crystal surface features have high roughness (hundreds of nanometers rms) inducing light scattering, SE cannot provide nanometric thickness measurement on this kind of substrate. SE was instead performed on the Si (100) witness sample. The stacking model is Si(100)/SiO_2 native oxide/TiO_2 with a SiO_2 native oxide thickness fixed at 2 nm.[52] The Tauc–Lorentz model[53,54] was used to determine TiO_2 properties. Because the material oscillator energy E_0

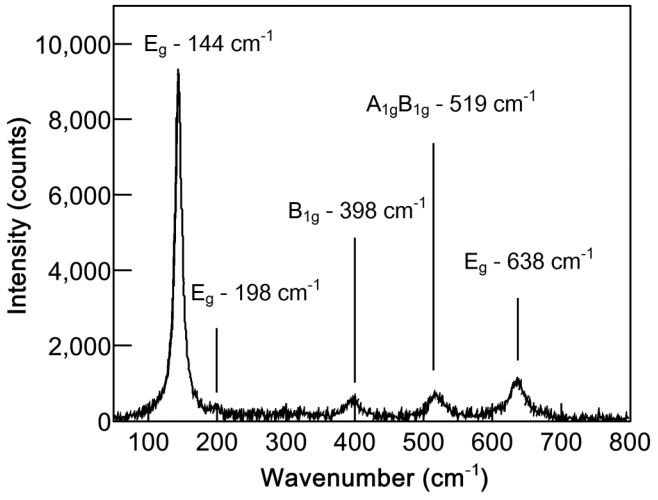

FIG. 4. Raman spectrum of 20-nm TiO_2 ALD coated QCM.

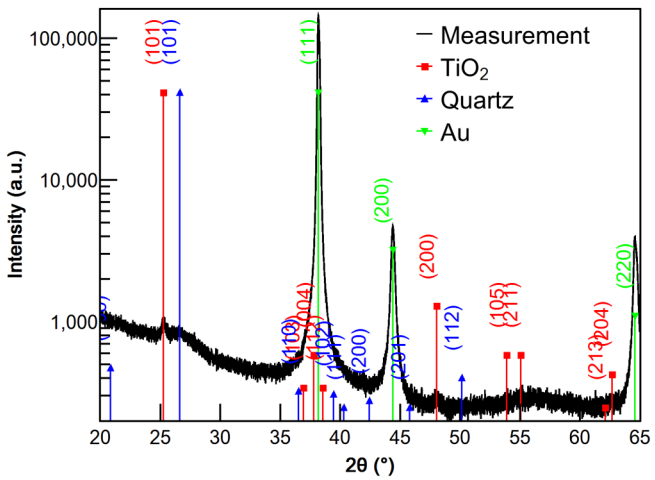

FIG. 5. Diffractogram of TiO_2 coated QCM at $\omega = 5°$.

lies outside the measurement range, it was fixed at 4.1 eV[55] for the adjustment with the dispersion model. The SE analysis yielded a thickness of 19.90 nm and a bandgap of 3.22 eV in agreement with 3.20 eV reported for anatase.[56,57] The refractive index of 2.60 at 550 nm is also in accordance with the reported value of 2.54.[58]

B. Photocatalytic experiment

The paraffin oil photocatalytic degradation experiment is reported in Fig. 7(a) in terms of thickness as a function of time. It can be divided into four phases: (1) the pumping phase from 0 to 0.33 h up to 1.6×10^{-6} mbar, (2) the contamination deposition between 0.33 and 0.44 h, (3) the air venting followed by a short temperature stabilization period between 0.47 and 0.81 h, and (4) the photocatalytic phase where UV irradiation is turned on between 0.81 and 2.22 h. The first phase (0–0.33 h) starts 20 min after turning on pumps in order to avoid a QCM thickness reading artifact coming from the possible pressure effect and the desorption of adsorbed ambient molecules (O_2, H_2O mainly). During this first phase, a small contamination intake close to 0.10 nm in thickness is attributed to a residual contamination coming from the outgassing of the vacuum chamber and its inner components. Such phenomenon is possible because QCMs are cooled at 15 °C, whereas the vacuum chamber is kept at ambient temperature close to 25 °C. After the deposition phase reported in Fig. 7(b), 10.0 nm was deposited on the QCM_1 and 7.5 nm on the QCM_2. Read QCM thickness is different from one QCM to the other in reason of their different view factors with respect to the contaminant source. Air venting is then performed inducing a sharp frequency shift due to a sudden change in pressure and temperature. In Fig. 7(a), this frequency shift is nevertheless translated into thickness but is considered to be a momentaneous measurement artifact. Air venting induces a QCM thickness reading shift from 10.0 nm to approximatively 15.1 nm and from 7.5 to 18.3 nm, respecively, for QCM_1 and QCM_2. Finally, after a short temperature stabilization, the illumination is turned on at 0.81 h. It instantaneously induces a frequency shift due to thermal changes and resulting stress in the quartz crystal.[59–62] The shift amplitude in the presented measurements is different from QCM_1 to QCM_2 because it depends on irradiance,[33,61–63] atmospheric composition,[62] QCM optical properties,[61–63] and its cut type.[59] Next, a clear mass decrease occurs for the TiO_2/Au-coated QCM while the mass remains stable for the Au-QCM. This decrease is attributed to the photocatalytic effect. Focusing on what is happening during irradiation allows to exclude the artifacts occuring during the other steps (air venting, turning on and off the irradiation, etc.). It can be seen than the deposited 10.0 nm is completely removed during irradiation while there is no mass change for QCM without TiO_2. During this period, QCM_1 read thickness goes from 11.5 to 1.5 nm while the QCM_2 remains at 19.9 nm. Since the paraffin loss corresponds to the amount originally deposited, namely, 10 nm, the remaining 1.5 nm read thickness is not a parrafin residue and is rather attributed to artifacts occuring between venting ($QCM_1 = 10.0$ nm at 0.47 h just before venting) and temperature stabilization at the beginning of illumination ($QCM_1 = 11.5$ nm at 0.84 h). They are induced by the sudden increase in pressure, temperature changes,

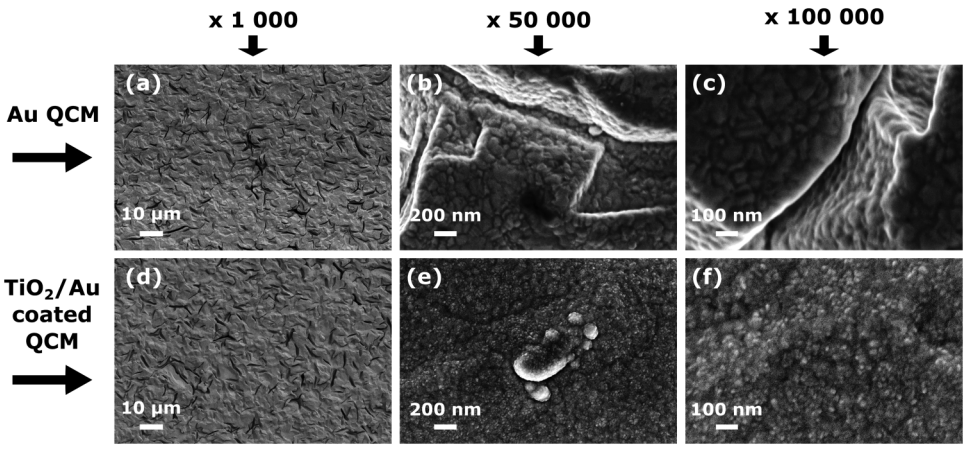

FIG. 6. SEM images of uncoated (a), (b), and (c) and TiO_2/Au-coated QCMs (d), (e), and (f) at low (a) and (d), middle (b) and (e), and high magnification (c) and (f).

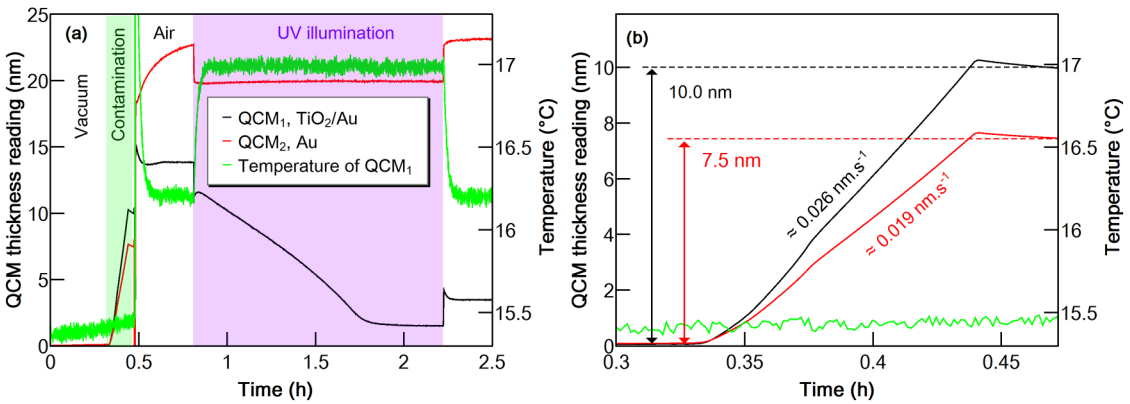

FIG. 7. (a) Overview of the full experiment comprising pumping, paraffin thin film deposition, venting, and photocatalytic decomposition; and (b) zoom in the paraffin thin film deposition phase.

and eventually interactions with species from air (adsorption, small flow on QCMs). At the end of the test, the QCM_1 read thickness reached 3.5 nm due to these artifacts plus the shift induced by illumination. Complete degradation was already observed by Minabe *et al.*[64] who characterized photocatalytic decomposition with 2.5 mg of paraffin oil over anatase TiO_2 synthesized by the pyrosol process with an electronic balance (precision of 10 μg equivalent to 4 nm for their 25-cm^2 sample considering a density of 1 g cm^{-3}). The present study confirms Minabe *et al.*'s results at a smaller scale. These results suggest that the reactant is completely converted into volatile products that do not condense on the TiO_2 surface after being produced. The formed products may be H_2O, CO_2, or other small molecules like light hydrocarbons. The complete degradation feature can be more easily appreciated in Fig. 8 (blue curve with triangle markers).

To ensure that the mass decrease could be attributed to a photocatalytic phenomenon, three other experiments were performed with an Au-coated QCM under UV illuminated in air, a TiO_2/Au-coated in air without UV, and a TiO_2/Au-coated QCM in N_2 again under UV illumination. In all cases, 10 nm of paraffin oil was deposited on the QCM_1 as explained in Sec. II B. A typical experiment is presented in Fig. 7 with the given conditions. Results are displayed in Fig. 8. For convenience, Fig. 8 shows paraffin thickness evolution during the illumination phase for 10 nm of deposited paraffin in each experience [purple rectangle in Fig. 7(a)]. Since no mass decrease is observed either on the TiO_2/Au-coated-QCM without UV and on the Au-coated QCM under UV, the mass loss observed with TiO_2/Au-coated QCM under irradiation is attributed to the photocatalytic self-cleaning effect. Moreover, it shows that there is no visible paraffin photolysis (at least inducing mass loss) or other phenomenon resulting from paraffin evaporation. The absence of photolysis could be expected since the contaminant has a low absorption coefficient with respect to the irradiation spectrum. Focusing now on the photocatalytic phenomenon, all the deposited paraffin oil is decomposed in approximatively 1 h when TiO_2/Au-coated-QCM is irradiated. The degradation process kinetics is close to have a zero order with a small inflexion in the last nanometers (Fig. 8). The latter may originate from contaminant morphological and/or viscoelastic property changes during the photocatalytic reaction modifying QCM resonance behavior and/or changes in the involved photocatalytic mechanism(s) (such as rate, reactions, intermediate products, available ROS species in TiO_2 vicinity, etc.). For example, the rate increase might be attributed to smaller paraffin thickness accelerating water and oxygen diffusion through it because of thin film discontinuities. Another explanation could be the direct charge transfer from TiO_2 to O_2/H_2O through the paraffin film becoming allowed or faster. In this last case and up to our knowledge, there is, however, no evidence of such behavior reported in the literature. The mass decrease being zero order-like, the linear part can be fitted to obtain a photocatalytic rate yielding

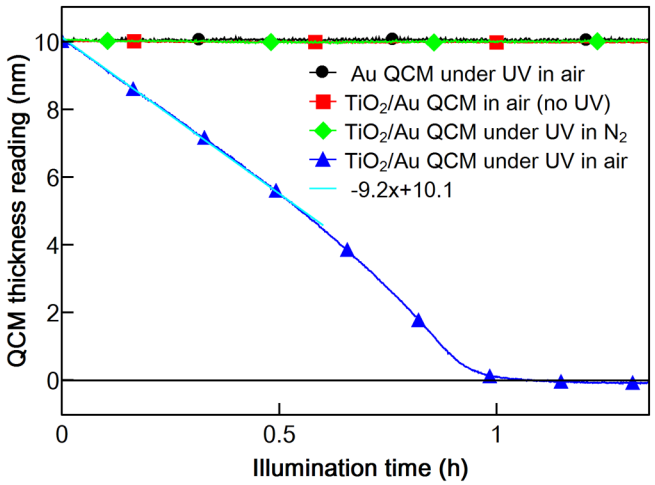

FIG. 8. QCM thickness reading for TiO_2/Au and Au QCM under different conditions highlighting the photocatalytic effect on the TiO_2/Au-coated QCM and its full contaminant removal during the illumination phase.

9.2 nm h^{-1}. Finally, when TiO_2 is exposed to UV in a N_2 atmosphere, no mass loss is observed. It suggests the involvement of H_2O and/or O_2 species in hydrocarbon decompositions. This observation can be expected since ROS are supposed to be the main vectors for photocatalytic redox reactions.[15] However, it does not demonstrate that H_2O and/or O_2 are, in absolute, indispensable. For such study, longer experiment and quantitative measurement of H_2O and O_2 would be required.

C. Equipment experiment opportunities

Thanks to the new setup, self-cleaning properties produced by photocatalysis can be easily characterized. Its versatility can lead to a wide range of experiments. With the effusion cell, both liquid and solid contaminants at room temperature can be used. The deposition into vacuum ensures smooth and precise deposition control from nanometers to hundreds of nanometers. It also reduces the extent of other potential mass contributions such as coming from the water adsorbed on TiO_2 or contained in the contaminant. Cooling the QCM keeps the samples at stable temperature drastically limiting the potential thermal desorption of contaminants. Thanks to the MgF_2 window wide band transparency and the external position of the illumination system, wavelength and flux dependencies can be easily studied by moving and changing irradiation sources or adding filters. The vacuum chamber features are suitable to provide controlled environment to perform experiments with different gas compositions and pressures.

The use of the QCM method allows to demonstrate the "true" self-cleaning effect by studying the contaminant mass on the QCM. Indeed, some other methods based on products' detection-like CO_2 by mass spectroscopy, UV-VIS spectroscopy, or contact angle measurement do not bring insights into the cleanliness level of the sample but only infer it since the contaminant itself is not characterized. In our opinion, the characterization method should be selected according to the objectives. For example, if the objective of self-cleaning is to keep high UV-VIS transmittance, transmission measurement over this spectral range would be a suitable method, but it would be less pertinent if the experiment aims to study the decontamination behavior as the loss of absorbance can originate from chromophore bond breaking without complete contaminant mineralization. Performing an experiment from the contamination phase up to self-cleaning under illumination has the advantage to reduce cross error due to sample handling. This is particularly suitable for a semiquantitative analysis and ageing tests with cycling. Moreover, the QCM method is also applicable for kinetic and self-cleaning behavior study even if interpretation must be done with care since temperature, stress, or viscoelastic changes affect the QCM frequency.

Finally, atomic layer deposition as a thin film deposition method is particularly appropriate for studying the efficiency of photocatalytic coatings with QCMs. First of all, due to high thin film uniformity and conformity provided by the technique on complex surfaces, QCMs rough surface can be more efficiently covered than with other deposition techniques such as sputtering. Moreover, quartz Curie temperature is approximatively 573 °C, but it can significantly be lowered by stress. Above it, quartz crystallographic structure changes and it loses its piezoelectric properties. Then, a practicable upper limit on the order of 300 °C for the deposition process would be recommended.[65] However, a specific crystalline phase is most of the time required to maximize or even support photocatalytic reactions. Such phases often require annealing at temperature higher than 300 °C (typically around 500 to 600 °C for anatase TiO_2). With ALD processes, the crystallization temperature is significantly lowered, making them suitable to QCM substrates in that respect and this is obviously not exclusive to TiO_2.

IV. CONCLUSIONS

With a new setup consisting of a vacuum chamber equipped with QCMs, an effusion cell, and an UV illumination system, we demonstrate a quick and easy method to characterize the real time self-cleaning properties of thin films. Thanks to ALD, we successfully functionalized QCM with 20 nm of anatase TiO_2 at relatively low temperature avoiding crystal substrate damage. After the deposition of a 10-nm paraffin oil thin film, the TiO_2 thin film shows a self-cleaning efficiency in ambient air under UV illumination of 9.2 nm h^{-1} ascribed to photocatalysis. A zero order-like kinetics is observed. Such an effect is not observed in N_2 atmosphere suggesting the prime importance of H_2O and O_2 for hydrocarbon decomposition. However, it does not establish that H_2O and O_2 are indispensable. Thanks to the new setup and method versatility, a wide range of studies can be performed with none or only a few modifications. It can address parameters such as gas nature and pressure, thin film thickness, and irradiation specificities with the targeted contaminant source. The ALD technique would allow the study of photocatalytic thin films with thicknesses ranging from a few to tens of nanometers with a sensitive substrate and conformal topography. The next experiments will aim at determining the effect of H_2O and O_2 species on self-cleaning from vacuum to ambient air partial pressures.

ACKNOWLEDGMENTS

The authors would especially like to thank Julien Rosin for his contribution to the experimental setup development and Frederic Wyczisk for taking parts in the TiO_2 coating analytical measurements.

REFERENCES

[1]O. Carp, Prog. Solid State Chem. **32**, 33 (2004).
[2]A. Fujishima, T. N. Rao, and D. A. Tryk, J. Photochem. Photobiol. C **1**, 1 (2000).
[3]A. Fujishima, X. Zhang, and D. Tryk, Surf. Sci. Rep. **63**, 515 (2008).
[4]A. Mills, C. Hill, and P. K. J. Robertson, J. Photochem. Photobiol. A **237**, 7 (2012).
[5]J.-M. Herrmann, Catal. Today **53**, 115 (1999).
[6]S. Malato, P. Fernández-Ibáñez, M. I. Maldonado, J. Blanco, and W. Gernjak, Catal. Today **147**, 1 (2009).
[7]J. Zhao and X. Yang, Build. Environ. **38**, 645 (2003).
[8]A. H. Mamaghani, F. Haghighat, and C.-S. Lee, Appl. Catal. B Environ. **203**, 247 (2017).
[9]J. Peral, X. Domènech, and D. F. Ollis, J. Chem. Technol. Biotechnol. **70**, 117 (1997).
[10]Z. Huang, P.-C. Maness, D. M. Blake, E. J. Wolfrum, S. L. Smolinski, and W. A. Jacoby, J. Photochem. Photobiol. A **130**, 163 (2000).
[11]R. Fagan, D. E. McCormack, D. D. Dionysiou, and S. C. Pillai, Mater. Sci. Semicond. Proc. **42**, 2 (2016).

[12]S. Banerjee, D. D. Dionysiou, and S. C. Pillai, Appl. Catal. B Environ. **176–177**, 396 (2015).
[13]A. Mills, S. Hodgen, and S. K. Lee, Res. Chem. Intermed. **31**, 295 (2005).
[14]L. Zhang, R. Dillert, D. Bahnemann, and M. Vormoor, Energy Environ. Sci. **5**, 7491 (2012).
[15]Y. Nosaka and A. Y. Nosaka, Chem. Rev. **117**, 11302 (2017).
[16]M. R. Hoffmann, S. T. Martin, Wonyong Choi, and D. W. Bahnemann, Chem. Rev. **95**, 69 (1995).
[17]A. Mills and S. Le Hunte, J. Photochem. Photobiol. A **108**, 1 (1997).
[18]D. M. Blake, *Bibliography of Work on the Heterogeneous Photocatalytic Removal of Hazardous Compounds From Water and Air* (National Renewable Energy Laboratory, Golden, CO, 1999).
[19]D. M. Blake, *Bibliography of Work on the Heterogeneous Photocatalytic Removal of Hazardous Compounds From Water and Air* (National Renewable Energy Laboratory, Golden, CO, 2001).
[20]D. S. Bhatkhande, V. G. Pangarkar, and A. A. Beenackers, J. Chem. Technol. Biotechnol. **77**, 102 (2002).
[21]R. Wang, K. Hashimoto, A. Fujishima, M. Chikuni, E. Kojima, A. Kitamura, M. Shimohigoshi, and T. Watanabe, Nature **388**, 431 (1997).
[22]R. Wang, K. Hashimoto, A. Fujishima, M. Chikuni, E. Kojima, A. Kitamura, M. Shimohigoshi, and T. Watanabe, Adv. Mater. **10**, 135 (1998).
[23]M. Miyauchi, A. Nakajima, T. Watanabe, and K. Hashimoto, Chem. Mater. **14**, 2812 (2002).
[24]*ISO 27448—Fine Ceramics (Advanced Ceramics, Advanced Technical Ceramics)—Test Method for Self-Cleaning Performance of Semiconducting Photocatalytic Materials—Measurement of Water Contact Angle* (International Organization for Standardization, Geneva, Switzerland, 2009).
[25]Z. Yang and C. Zhang, J. Mol. Catal. A-Chem. **302**, 107 (2009).
[26]Z. Yang, J. Yan, C. Zhang, and S. Luo, Colloid. Surf. B **87**, 187 (2011).
[27]H. Hidaka, H. Honjo, S. Horikoshi, and N. Serpone, New J. Chem. **27**, 1371 (2003).
[28]I. Iñarritu, E. Torres, A. Topete, and J. Campos-Terán, J. Colloid Interface Sci. **506**, 36 (2017).
[29]M. Miller, W. E. Robinson, A. R. Oliveira, N. Heidary, N. Kornienko, J. Warnan, I. A. C. Pereira, and E. Reisner, Angew. Chem. Int. Ed. **58**, 4601 (2019).
[30]Z. Yang and C. Zhang, Catal. Commun. **10**, 351 (2008).
[31]Y. Nakamura, Y. Katou, and S. Rengakuji, Electrochemistry **72**, 408 (2004).
[32]P. Chin, C. S. Grant, and D. F. Ollis, Appl. Catal. B Environ. **87**, 220 (2009).
[33]T. Abe and H. Kato, J. Micromech. Microeng. **19**, 094019 (2009).
[34]W. Qiang, L. Wei, W. Shaodan, and B. Yu, Appl. Surf. Sci. **347**, 755 (2015).
[35]J. Joo, D. Lee, M. Yoo, and S. Jeon, Sensor. Actuat. B-Chem. **138**, 485 (2009).
[36]F. Rupp *et al.*, J. Dent. Res. **91**, 104 (2012).
[37]T. Kallio, S. Alajoki, V. Pore, M. Ritala, J. Laine, M. Leskelä, and P. Stenius, Colloid. Surf. A **291**, 162 (2006).
[38]F. Rupp *et al.*, Acta Biomater. **6**, 4566 (2010).
[39]Y. Wu, J. Geis-Gerstorfer, L. Scheideler, and F. Rupp, Biofouling **32**, 583 (2016).
[40]R. Norman Jones, Chem. Rev. **32**, 1 (1943).
[41]V. Miikkulainen, M. Leskelä, M. Ritala, and R. L. Puurunen, J. Appl. Phys. **113**, 021301 (2013).
[42]J. Bachmann, *Atomic Layer Deposition in Energy Conversion Applications* (Wiley-VCH Verlag GmbH & Co. KGaA, Weinheim, 2017).
[43]S. M. George, Chem. Rev. **110**, 111 (2010).
[44]Kurt J. Lesker Company, Material Deposition Chart, see: https://www.Lesker.Com/Newweb/Deposition_materials/Materialdepositionchart.Cfm?Pgid=0.
[45]C. Lu and O. Lewis, J. Appl. Phys. **43**, 4385 (1972).
[46]C. Lu, J. Vac. Sci. Technol. **12**, 578 (1975).
[47]A. Wajid, Rev. Sci. Instrum. **62**, 2026 (1991).
[48]E. Benes, J. Appl. Phys. **56**, 608 (1984).
[49]K. H. Behrndt, J. Vac. Sci. Technol. **8**, 622 (1971).
[50]X. Chen and S. S. Mao, Chem. Rev. **107**, 2891 (2007).
[51]T. Ohsaka, F. Izumi, and Y. Fujiki, J. Raman Spectrosc. **7**, 321 (1978).
[52]A. H. Al-Bayati, K. G. Orrman-Rossiter, J. A. van den Berg, and D. G. Armour, Surf. Sci. Lett. **241**, A5 (1991).
[53]G. E. Jellison and F. A. Modine, Appl. Phys. Lett. **69**, 371 (1996).
[54]G. E. Jellison and F. A. Modine, Appl. Phys. Lett. **69**, 2137 (1996).
[55]H. Tang, H. Berger, P. E. Schmid, and F. Lévy, Solid State Commun. **92**, 267 (1994).
[56]D. O. Scanlon *et al.*, Nat. Mater. **12**, 798 (2013).
[57]H. Tang, K. Prasad, R. Sanjinès, P. E. Schmid, and F. Lévy, J. Appl. Phys. **75**, 2042 (1994).
[58]T. Jones and T. A. Egerton, in *Kirk-Othmer Encyclopedia of Chemical Technology*, edited by John Wiley & Sons, Inc. (Wiley, Hoboken, NJ, 2012).
[59]D. A. Wallace, S. A. Wallace, and K. W. Rogers, in *Optical Systems Contamination and Degradation*, edited by P. T. C. Chen, W. E. McClintock, and G. J. Rottman (International Society for Optics and Photonics, San Diego, CA, 1998), Vol. 3427, pp. 76–87, available at https://www.spiedigitallibrary.org/conference-proceedings-of-spie/3427/1/First-tests-of-an-extremely-high-mass-sensitivity--miniature/10.1117/12.328522.short?SSO=1.
[60]L. H. Goodman, E. S. Bililign, B. W. Keller, S. G. Kenny, and J. Krim, J. Appl. Phys. **124**, 024502 (2018).
[61]Y. Zong, F. Xu, X. Su, and W. Knoll, J. Appl. Phys. **103**, 104503 (2008).
[62]T. Kawasaki, T. Mochida, J. Katada, and Y. Okahata, Anal. Sci. **25**, 1069 (2009).
[63]A. Fomin, M. Poliak, V. Tsionsky, S. Cheskis, and I. Rahinov, Sensor. Actuat. B-Chem. **202**, 861 (2014).
[64]T. Minabe, D. A. Tryk, P. Sawunyama, Y. Kikuchi, K. Hashimoto, and A. Fujishima, J. Photochem. Photobiol. A **137**, 53 (2000).
[65]*Temperature Coefficient of Maxtek Monitor Crystals* (Inficon, 2005), available at https://products.inficon.com/getattachment.axd/?attaName=d2c92a2a-c4ab-49fa-8e55-45b59bbc8f7b.